Published in final edited form as:
Nature. 2015 January 1; 517(7532): 89–93. doi:10.1038/nature13801.

Human intracellular ISG15 prevents interferon-α/β over-amplification and auto-inflammation

Xianqin Zhang[1,*], **Dusan Bogunovic**[2,3,*], **Béatrice Payelle-Brogard**[4,*], **Véronique Francois-Newton**[4,*], **Scott D. Speer**[3,5,6], **Chao Yuan**[1], **Stefano Volpi**[7,8], **Zhi Li**[4], **Ozden Sanal**[9], **Davood Mansouri**[10], **Ilhan Tezcan**[9], **Gillian I. Rice**[11], **Chunyuan Chen**[12], **Nahal Mansouri**[10], **Seyed Alireza Mahdaviani**[10], **Yuval Itan**[2], **Bertrand Boisson**[2], **Satoshi Okada**[2], **Lu Zeng**[1], **Xing Wang**[1], **Hui Jiang**[13], **Wenqiang Liu**[1], **Tiantian Han**[1], **Delin Liu**[14], **Tao Ma**[1], **Bo Wang**[15], **Mugen Liu**[1], **Jing-Yu Liu**[1], **Qing K. Wang**[1,16], **Dilek Yalnizoglu**[9], **Lilliana Radoshevich**[17], **Gilles Uzé**[18], **Philippe Gros**[19], **Flore Rozenberg**[20], **Shen-Ying Zhang**[2], **Emmanuelle Jouanguy**[21,22], **Jacinta Bustamante**[21,22,23], **Adolfo Garcìa-Sastre**[3,5,24], **Laurent Abel**[2,21,22], **Pierre Lebon**[20], **Luigi D. Notarangelo**[7], **Yanick J. Crow**[11,22,25], **Stèphanie Boisson-Dupuis**[2,21,22], **Jean-Laurent Casanova**[21,22,26,27,§], and **Sandra Pellegrini**[4,§]

[1]Key Laboratory of Molecular Biophysics of the Ministry of Education, College of Life Science and Technology, Huazhong University of Science and Technology, Wuhan 430074, China

[2]St. Giles Laboratory of Human Genetics of Infectious Diseases, Rockefeller Branch, The Rockefeller University, New York, New York 10065, USA

[3]Department of Microbiology, Icahn School of Medicine at Mount Sinai, New York, New York 10029, USA

[4]Institut Pasteur, Cytokine Signaling Unit, CNRS URA 1961, 75724 Paris, France

[5]Global Health and Emerging Pathogens Institute, Icahn School of Medicine at Mount Sinai, New York, New York 10029, USA

[6]Microbiology Training Area, Graduate School of Biomedical Sciences of Icahn School of Medicine at Mount Sinai, New York, New York 10029, USA

[7]Division of Immunology, Children's Hospital Boston, Boston, Massachusetts 02115, USA

[8]Department of Neuroscience, Rehabilitation, Ophthalmology, Genetics, Maternal and Child Health, University of Genoa, 16132 Genoa, Italy

---

Correspondence and requests for materials should be addressed to D.B. (Dusan.Bogunovic@mssm.edu).
*These authors contributed equally to this work.
§These authors jointly supervised this work.

Online Content Methods, along with any additional Extended Data display items and Source Data, are available in the online version of the paper; references unique to these sections appear only in the online paper.

Supplementary Information is available in the online version of the paper.

Author Contributions D.B., X.Z., B.P.-B., V.F.-N., O.S., D.M., P.G., A.G.-S., L.A., P.L., L.D.N., S.B.-D., Y.J.C., J.-L.C. and S.P. wrote the manuscript. D.B., X.Z., B.P.-B., V.F.-N., S.D.S., C.Y., S.V., Z.L., I.T., G.I.R., C.C., N.M., S.A.M., Y.I., B.B., S.O., L.Z., X.W., H.J., W.L., T.H., D.L., T.M., B.W., D.Y., L.R., G.U., P.G., F.R., S.-Y.Z., E.J., J.B., A.G.-S., L.A., P.L., L.D.N., S.B.-D., Y.J.C., J.-L.C. and S.P. designed and/or performed experiments. M.L., J.-Y.L., Q.K.W., O.S., D.M., N.M., I.T. and S.A.M. took clinical care of the patients and provided advice.

The authors declare no competing financial interests. Readers are welcome to comment on the online version of the paper.

[9]Immunology Division and Pediatric Neurology Department, Hacettepe University Children's Hospital, 06100 Ankara, Turkey

[10]Division of Infectious Diseases and Clinical Immunology, Pediatric Respiratory Diseases Research Center, National Research Institute of Tuberculosis and Lung Diseases, Shahid Beheshti University of Medical Sciences, 4739 Teheran, Iran

[11]Manchester Academic Health Science Centre, University of Manchester, Genetic Medicine, Manchester, M13 9NT, UK

[12]Department of Pediatrics, Third Xiangya Hospital, Central South University, Changsha 410013, China

[13]BGI-Shenzhen, Shenzhen 518083, China

[14]Sangzhi County People's Hospital, Sangzhi 427100, China

[15]Genetics Laboratory, Hubei Maternal and Child Health Hospital, Wuhan, Hubei 430070, China

[16]Center for Cardiovascular Genetics, Department of Molecular Cardiology, Lerner Research Institute, Cleveland Clinic, Cleveland, Ohio 44195, USA

[17]Institut Pasteur, Bacteria-Cell Interactions Unit, 75724 Paris, France

[18]CNRS UMR5235, Montpellier II University, Place Eugène Bataillon, 34095 Montpellier, France

[19]Department of Biochemistry, McGill University, Montreal, QC H3A 0G4, Canada

[20]Paris Descartes University, 75006 Paris, France

[21]Laboratory of Human Genetics of Infectious Diseases, Necker Branch, INSERM U1163, Necker Hospital for Sick Children, 75015 Paris, France

[22]Paris Descartes University, Imagine Institute, 75015 Paris, France

[23]Center for the Study of Primary Immunodeficiencies, Necker Hospital for Sick Children, 75015 Paris, France

[24]Department of Medicine, Division of Infectious Diseases, Icahn School of Medicine at Mount Sinai, New York, New York 10029, USA

[25]INSERM UMR 1163, Laboratory of Neurogenetics and Neuroinflammation, Imagine Institute, 75006 Paris, France

[26]Howard Hughes Medical Institute, New York, New York 10065, USA

[27]Pediatric Hematology–Immunology Unit, Necker Hospital for Sick Children, 75015 Paris, France

Abstract

Intracellular ISG15 is an interferon (IFN)-α/β-inducible ubiquitin-like modifier which can covalently bind other proteins in a process called ISGylation; it is an effector of IFN-α/β-dependent antiviral immunity in mice[1–4]. We previously published a study describing humans with inherited ISG15 deficiency but without unusually severe viral diseases[5]. We showed that these patients were prone to mycobacterial disease and that human ISG15 was non-redundant as an extracellular IFN-γ-inducing molecule. We show here that ISG15-deficient patients also

display unanticipated cellular, immunological and clinical signs of enhanced IFN-α/β immunity, reminiscent of the Mendelian autoinflammatory interferonopathies Aicardi–Goutières syndrome and spondyloenchondrodysplasia[6–9].We further show that an absence of intracellular ISG15 in the patients' cells prevents the accumulation of USP18[10,11], a potent negative regulator of IFN-α/β signalling, resulting in the enhancement and amplification of IFN-α/β responses. Human ISG15, therefore, is not only redundant for antiviral immunity, but is a key negative regulator of IFN-α/β immunity. In humans, intracellular ISG15 is IFN-α/β-inducible not to serve as a substrate for ISGylation-dependent antiviral immunity, but to ensure USP18-dependent regulation of IFN-α/β and prevention of IFN-α/β-dependent autoinflammation.

Calcification of the cerebral basal ganglia during childhood is an important radiological sign associated with a range of genetic and non-genetic states[12,13]. In Fahr's disease, also known as idiopathic basal ganglia calcification (IBGC)[14–17], the genetic causes identified are germline mutations of the *SLC20A2, PDGFB* and *PDGFRB* genes[15,16]. Intracranial calcification is also a well recognized feature of a group of Mendelian autoinflammatory diseases associated with upregulation of IFN-α/β signalling[8,18], including Aicardi–Goutières syndrome (AGS) and spon-dyloenchondromatosis (SPENCD), in particular. We investigated three siblings from China with IBGC. The eldest child (P4) died during an episode of epileptic seizures at the age of 13 years (Supplementary Information, case report). The other two siblings, currently aged 11 (P6) and 13 (P5) years, have suffered only occasional seizures. Despite having been exposed to common childhood viruses (Extended Data Table 1), these children have experienced no severe infectious disease. Whole-exome sequencing (WES) of P5 and P6 and their healthy mother identified only one common nonsense homozygous mutation, which had not been reported in public databases or in in-house WES data for 1,500 other individuals (Extended Data Table 2). This variant was in exon 2 of *ISG15*: c.163C>T/163C>T (p.Gln 55*/Gln 55*; asterisks denote stop codons). Familial segregation was consistent with an autosomal recessive mode of inheritance (Fig. 1a, b and Extended Data Fig. 1a).

This observation was surprising, as we recently described three unrelated children from two families from Turkey and Iran who were homozygous for loss-of-function mutations of *ISG15*[5]. These patients (P1, P2 and P3, now aged 17, 14 and 17 years, respectively) displayed clinical disease caused by the BCG vaccine, which, in otherwise healthy individuals, defines Mendelian susceptibility to mycobacterial disease (MSMD), a rare disorder characterized by severe clinical disease following infection with weakly virulent mycobacteria[19,20]. In these patients, MSMD resulted from insufficient ISG15-dependent IFN-γ production[21]. These patients displayed no severe viral disease[2]. Following the identification of *ISG15* mutations in Chinese children with a putative diagnosis of IBGC, we performed computed tomography (CT) scans on the Iranian and Turkish ISG15-deficient MSMD patients. We found that P1 and P2 displayed calcification of the basal ganglia, with CT imaging in P3 also showing calcification along the cerebral falx (Fig. 1c).The ISG15-deficient patients from China were not vaccinated with BCG at birth, consistent with their current lack of an MSMD phenotype. The c.163C>T/163C>T mutant allele showed no ISG15 protein on western blots (Extended Data Fig. 1b). In total, six patients (P4 with inferred genotype) with IBGC from three kindreds from China, Iran and Turkey were found

to have only homozygous rare and null *ISG15* mutant alleles in common (Extended Data Table 3). These findings strongly suggest that the three *ISG15* alleles identified are disease-causing, not only for MSMD, but also for IBGC, an intracranial calcification phenotype unrelated to any obvious cerebral infection.

We next investigated whether enhanced IFN-α/β immunity might account for both the lack of antiviral immunodeficiency[5] and the intracranial calcification, as in patients with autoinflammatory AGS and SPENCD[18]. AGS- and SPENCD-causing mutations can lead to high levels of IFN-α/β in the blood and cerebrospinal fluid, and an upregulation of interferon-stimulated genes[9]. Such an IFN-α/β signature is also observed in patients with the autoimmune disorder systemic lupus erythematosus (SLE), which is sometimes associated with basal ganglia calcification and may be allelic with AGS in rare cases[6,22,23]. We determined the expression levels of six interferon-stimulated genes reported to be upregulated in patients with AGS[7]. *IFI27, IFI44L, IFIT1, ISG15, RSAD2* and *SIGLEC1* transcripts were measured in peripheral blood or peripheral blood mononuclear cells from ISG15-deficient patients and controls. Notably, all ISG15-deficient patients, like patients with AGS, had significantly higher levels of interferon-stimulated gene messenger RNA than unaffected relatives or healthy controls (Fig. 2a). The two Chinese patients who displayed seizures (P5 and P6) also had detectable IFN-α antiviral activity in their plasma (Extended Data Fig. 1c, d). These findings indicate that the constitutive enhancement of IFN-α/β activity characterizes ISG15 deficiency, in addition to AGS and SPENCD. All three of these conditions have the same prominent radiological sign, intracranial calcification.

ISG15 is an IFN-α/β-inducible ubiquitin-like protein that can be conjugated to many intracellular substrates via ISGylation[1,3,4,24–26]; we wondered how and why ISG15 deficiency would be associated with enhanced IFN-α/β immunity. We investigated the relationship between ISG15 deficiency and enhanced IFN-α/β immunity by monitoring the IFN-α response of hTert-immortalized fibroblasts from P1, P2, P3 and controls by reverse transcription with quantitative PCR (RT–qPCR) and genome-wide microarray analyses (Fig. 2b, c and Extended Data Table 4). The relative levels of 78 transcripts, including 20 canonical interferon-stimulated genes (including *RSAD2, IFI27, OAS3, IFI44, USP18, IFIT1* and *MX1*; Extended Data Table 4) were significantly higher in patients than in controls. This *in vitro* phenotype was rescued by transduction with wild-type *ISG15* (Fig. 2d) or with *ISG15* (Δ*GG*), a mutant incapable of conjugation (Extended Data Fig. 2a)[5].We excluded the involvement of secreted ISG15 (Extended Data Fig. 2b). Consistent with mRNA levels, cells from patients expressedmoreMX1 and IFIT1 proteins than control cells (Fig. 3a, b). Remarkably, however, levels of USP18 were low in patients' cells (Fig. 3a, b), despite their higher levels of *USP18* mRNA (Fig. 2c and Extended Data Table 4). Similar data were obtained for patient-derived Epstein–Barr virus (EBV)-transformed B cells and Simian virus 40 (SV40)-transformed cell lines, as well as for fibrosarcoma cells (HLLR1-1.4) and a human epithelial cell line, WISH, in which *ISG15* was silenced (Extended Data Fig. 3a, b, c). These results demonstrate a positive impact of ISG15 deficiency on the IFN-α/β response and suggest the possible involvement of USP18.

USP18 is an interferon-stimulated gene, an isopeptidase and a potent negative regulator of IFN-α signalling[10,27,28]. We therefore hypothesized that, in the absence of ISG15, IFN-α/β

signalling would be inadequately attenuated due to insufficient USP18. Indeed, in patients' cells, STAT1 and STAT2 were more persistently phosphorylated and IFIT1 andMX1 levels were higher than in controls, whereas USP18 levels were low (Fig. 3a, b and Extended Data Fig. 3a). The same was observed following the knockdown of *USP18* and/or *ISG15* expression in HLLR1-1.4 cells primed with IFN-β (Fig. 3c). ISG15 appeared to act in its unconjugated free form, since silencing of *UBE1L* or of other ISGylation enzymes failed to reduce USP18 levels (Fig. 3d and Extended Data Fig. 3d) and patients' cells transduced with wild-type *ISG15* or *ISG15* (Δ*GG*) exhibited attenuated levels of interferon-stimulated-gene transcripts and proteins (Extended Data Fig. 2a and Fig. 3e). These data indicate that intracellular free ISG15 downregulates the IFN-α/β response by maintaining levels of the negative-feedback regulator USP18.

We then investigated the mechanism by which ISG15 regulates USP18. We measured the translation-independent decay of USP18 in hTert fibroblasts. In cells lacking ISG15, unlike control cells, USP18 levels began to decline after as little as one hour of cycloheximide (CHX) treatment (Fig. 4a and Extended Data Fig. 4a, b). This phenotype was reversed by transduction of patients' cells with wild-type *ISG15* or *ISG15* (Δ*GG*) constructs (Fig. 4b and Extended Data Fig. 4c). In HEK293T cells, co-transfection of *USP18* with either wild-type *ISG15* or *ISG15* (Δ*GG*) resulted in augmented USP18 protein levels (Fig. 4c). Co-transfection of *USP18* with ubiquitin led to strong ubiquitination of USP18 (Fig. 4d, lane 5 and Extended Data Fig. 4d), as previously reported[11]. The coexpression of either wild-type *ISG15* or *ISG15* (Δ*GG*) with *USP18* and ubiquitin resulted in markedly lower levels of USP18 ubiquitination (Fig. 4d, lanes 9–11 and Extended Data Fig. 4e) and larger total amounts of USP18.Overall, these data indicate that free intracellular ISG15 antagonizes USP18 ubiquitination and degradation, thereby promoting the stability and function of this protein.

USP18 is subject to S-phase kinase-associated protein 2 (SKP2)-mediated proteolysis[11,29]. We therefore analysed the impact of ISG15 on SKP2-mediated USP18 degradation. The formation of the USP18–SKP2 complex (Fig. 4e, lane 8), was prevented by co-expression of ISG15 (lane 10 versus lane 8) and ISG15 co-immunoprecipitated with USP18 independently of SKP2 expression (lanes 9 and 10). Finally, we assessed IFN-induced USP18 accumulation in cells silenced for SKP2. At 24 h and beyond, USP18 levels were higher in SKP2-silenced than in unsilenced cells (Fig. 4f and Extended Data Fig. 4f). These results suggest that ISG15 can antagonize SKP2-mediated proteolysis of USP18, although the involvement of other E3 ligases cannot be excluded. In the absence of ISG15, USP18 proteolysis is more rapid, driving the dysregulated IFN-α/β response and resulting in both the blood IFN-α/β signature and brain calcifications seen in the patients.

In conclusion, we have shown that all six ISG15-deficient children identified to date display abnormally strong IFN-α/β immunity, as demonstrated by their high levels of circulating IFN-α and/or leukocyte interferon-stimulated genes. As in patients with AGS and SPENCD[30], ISG15-deficient individuals display marked intracranial calcification. Three of the six ISG15-deficient individuals experienced epileptic seizures, which were lethal in one case. These patients also had autoantibody levels higher than those in age-matched controls (Extended Data Fig. 5). We found that ISG15 deficiency led to reduced levels of the

negative regulator USP18 because of increased proteolysis due, at least in part, to SKP2-mediated ubiquitination, resulting in stronger responses to IFN-α/β and an ensuing amplification of IFN-α/β-induced responses. The observed enhancement of cellular responses to IFN-α/β provides an explanation for the lack of overt viral infection phenotypes in patients with ISG15 deficiency[5]. More importantly, human ISG15 is not only redundant for antiviral immunity in these patients, it is a key negative regulator of IFN-α/β. The role of ISG15 in stabilizing USP18 is essential and independent of conjugation. We have not tested whether ISGylated proteins might also stabilize USP18. The broad susceptibility to viral infections of ISG15-deficient mice[2] but not humans[21] may be due to different biochemical properties of murine versus human ISG15 and/or USP18, affecting their interaction potential. Simultaneously, the lack of free extracellular ISG15 resulted in lower IFN-γ production by lymphocytes, thereby underlying MSMD in these patients[5].The phenotypic dichotomy of this monogenic disease, with both autoimmunity and MSMD, probably reflects the functional dichotomy of intracellular versus extracellular ISG15, respectively. There is currently no evidence that IFN-α/β-inducible human intracellular ISG15 exerts antiviral effects on documented viral infections via ISGylation. On the contrary, we show that IFN-α/β-inducible ISG15 is essential to negatively regulate IFN-α/β responses via USP18 stabilization, thereby preventing autoinflammatory consequences of uncontrolled IFN-α/β amplification.

METHODS

Exome capture, sequencing, alignments and variant calling

Exome sequencing was performed on two affected sisters and their unaffected mother. Libraries were prepared following the kit manufacturer's protocol. In brief, we randomly fragmented 3 μg of purified genomic DNA with an ultrasonoscope (Covaris, Massachusetts, USA) to produce fragments of 150~200 base pairs (bp) in length. The shotgun library was then subjected to hybridization with the Agilent SureSelect Human All Exon 50Mb kit (Agilent Technologies, California, USA) for exome capture, followed by several cycles of amplification before quality control with a 2100 Bioanalyzer (Agilent Technologies) and quantification by RT–qPCR with the StepOnePlus Real-Time PCR System (Life Technologies, California, USA). The final library was sequenced on an Illumina Hiseq2000 (Illumina, California, USA) with 90-bp paired-end reads, following the Hiseq2000 protocol. We used BWA Aligner to align the sequences with the human genome reference sequence (hg18 build). Downstream processing was carried out with the Genome analysis toolkit (GATK) SAMtools and Picard Tools (http://picard.sourceforge.net). Substitution calls were made with a GATK Unified Genotyper, whereas insertion/deletion (indel) calls were made with a GATK Indel GenotyperV2. All calls with a read coverage ≤2× and a Phred-scaled SNP quality ≤20 were filtered out. All the variants were annotated with the GATK Genomic Annotator. For filtering purposes, we used the 1000 Genomes and EVS databases, and an in-house exome database containing data for over 1,000 individuals. For the comparative analysis of P1, P2, P5 and P6, we removed variants with less than six reads and a mapping quality of less than 40 (per GATK), and we used the dbSNP database in addition to the 1000 Genomes and EVS databases.

qPCR and microarray analysis

We assessed the expression of six known interferon-stimulated genes in whole blood. Total RNA was extracted from whole blood with the PAXgene (PreAnalytix) RNA isolation kit. RNA concentration was assessed with a spectrophotometer (FLUOstar Omega, Labtech). Quantitative reverse transcription PCR analysis was performed with the *Taq*Man Universal PCR Master Mix (Applied Biosystems) and cDNA derived from40 ng of total RNA. The relative abundance of target transcripts, measured with *Taq*Man probes for *IFI27* (Hs01086370_m1), *IFI44L* (Hs00199115_m1), *IFIT1* (Hs00356631_g1), *ISG15* (Hs00192713_m1), *RSAD2* (Hs01057264_m1), and *SIGLEC1* (Hs00988063_m1), was normalized with respect to the expression of *HPRT1* (Hs03929096_g1) and *18S* (Hs999999001_s1) and assessed with Applied Biosystems StepOne Software v2.1 and Applied Biosystems Data Assist Software v3.01. Data for the patients are expressed relative to mean values for 23 normal controls. For PBMCs, total RNA was extracted with the RNeasy Mini kit (Qiagen). It was not possible to standardize the amount of RNA added to the cDNA synthesis reaction, but expression was nonetheless normalized with respect to the level of expression of *HPRT1* (Hs03929096_g1) and *18S* (Hs999999001_s1). For PBMCs and hTert fibroblasts, total RNA was extracted with the RNeasy Mini kit (Qiagen) and the standard protocol for hybridization to Affymetrix HTA 2.0 chips was performed. In microarray experiments, we used 1,000 IU ml^{-1} IFN-α2b as a stimulus. Affymetrix Expression Console and Transcriptome Analysis Console were used for analysis. Upregulation or downregulation was defined as significant if expression was twofold higher or lower for P1, P2 and P3 IFN-α2b-stimulated cells than for C1, C6 and C18 IFN-α2b-stimulated cells.

Cell lines and reagents

Human fibrosarcoma HLLR1-1.4 cells, which have been described elsewhere[25], were cultured in Dulbecco'smodified Eagle's medium(DMEM) (Gibco) supplemented with 10% fetal calf serum, hypoxanthine, thymidine and aminopterin (HAT) and 400 μg ml^{-1} G418 (Gibco). WISH amnion-derived epithelial cells, HEK293T cells, SV40-transformed and hTert-immortalized fibroblasts from controls and patients were cultured in DMEM supplemented with 10% fetal calf serum. EBV-transformed B cells from patient P1 and controls were cultured in RPMI medium supplemented with 10% fetal calf serum. Recombinant IFN-α2b was a gift from D. Gewert (Wellcome Foundation, Beckenham, Kent, UK; now at BioLauncher Ltd, Cambridge, UK) or was purchased from Schering; IFN-β was obtained from Biogen Idec, Cambridge, MA, USA. IFNs were purified to specific activities of $>10^8$ units per mg of protein. Cycloheximide (CHX) (Sigma) was used at a concentration of 20 μg ml^{-1}.

Plasmids and transfection

HEK293T cells were transiently transfected with the FuGENE6 system (Roche Applied Science). The pMET7-USP18 expression vector has been described elsewhere[27]; pcDNA3+ His_6-3×FlagISG15 (Fig. 4d, e and Extended Data Fig. 4d) was provided by J. M. Huibregtse (University of Texas at Austin, TX, USA), pBabe-3×Flag6His-ISG15 (BUG3354) and pBabe-3×Flag6His-ISG15(ΔGG) (BUG3355) (Fig.4c and Extended Data Fig. 4e) were

derived from this plasmid; pcDNA3 Flag–SKP2 and HA–ubiquitin constructs were obtained from E. Bianchi (Institut Pasteur, Paris, France). In co-transfection experiments, empty vector was added to keep the total amount of DNA constant.

siRNA-mediated silencing

USP18, UBE1L, UbcH8, HERC5, SKP2 ON-TARGET plus SMART pools and a control siRNA (ON-TARGET plus non-targeting pool) were obtained from Dharmacon. Three individual *ISG15*-targeting siRNAs from Sigma were tested: *ISG15#9*, GGACAAAUGCGACGAACCU; *ISG15#11*, GCAGAUCA CCCAGAAGAUU; *ISG15#12*, GCAACGAAUUCCAGGUGUC. All efficiently targeted *ISG15* transcripts. In all the experiments shown, *ISG15#12* was used. Cells were transfected with 25 nM siRNA for 24 h in the presence of the Lipofectamine RNAi max reagent (Invitrogen), according to the manufacturer's instructions. Cells were then stimulated with IFN.

Protein analyses

Cells were lysed in modified RIPA buffer (50 mM Tris/HClpH8, 200 mM NaCl, 1% Nonidet P40, 0.5% deoxycholate, 0.05% SDS, 2 mM EDTA), 1 mM orthovanadate and a protease inhibitor cocktail and subjected to western blotting. For co-immunoprecipitation, cells were lysed in 50 mM Tris, pH 6.8, 0.5% Nonidet P40, 200 mM NaCl, 10% glycerol, 1 mM EDTA and a protease inhibitor cocktail. For the analysis of USP18 ubiquitination (Fig. 4d and Extended Data Fig. 4d and 4e), cells were lysed in modified RIPA buffer and a protease inhibitor cocktail, and USP18 was immunoprecipitated from post-nuclear lysates for 2 h at 4 °C. It was then subjected to protein A capture and western blotting. The antibodies used were directed against STAT1 and STAT2 (Millipore), phospho-Tyr 701 STAT1 (Cell Signaling Technology), phospho-Tyr 689 STAT2 (Millipore), USP18 and AKT (Cell Signaling Technology), actin (Sigma), p27 (Santa Cruz Biotechnology), SKP2 (Invitrogen), HA (Santa Cruz Biotechnology), ISG15 (a gift from E. C. Borden, Cleveland Clinic, Cleveland, OH, USA or purchased from ABGENT, no. AP1150a), IFIT1 (a gift from G. Sen, Cleveland Clinic, Cleveland, OH, USA), OAS2 p69 (a gift from A. Hovanessian, Universitè Paris-Descartes, Paris, France), MxA (a gift from O. Haller, University of Freiburg, Freiburg, Germany) and ubiquitin (clone FK2 recognizing mono- and poly-ubiquitinated proteins, Enzo Life Sciences). An enhanced chemilum-inescence detection reagent was used for detection (Western Lightning, Perkin Elmer). Relative band intensities were measured with a Fuji ImageQuant LAS-4000.

Statistics

For larger samples there is a normal distribution, while for smaller samples (for example, $n = 2$) a distribution cannot be established. For larger samples there is a normal variance, while for smaller samples (for example, $n = 2$) variance cannot be established. Statistical methods used were defined in the legends of the figures where appropriate.

Autoantibody detection

Screening for a broad panel of IgG and IgA autoantibodies was performed with autoantibody arrays (University of Texas Southwestern Medical Center, Genomic and

Microarray Core Facility), as previously described[31]. In brief, diluted serum samples were incubated in duplicate with the autoantigen array and the autoantibodies binding to the antigens were detected with Cy3 and Cy5 fluorescent labelled anti-Ig antibodies (IgG and IgA), by the generation of TIFF images. Genepix Pro 6.0 software was used to analyse the images. Net fluorescence intensities (defined as fluorescence intensity for the spot minus background fluorescence intensity) for duplicate spots were averaged. The signal-to-noise ratio (SNR) was used as a quantitative measurement of the ability to resolve true signal from background noise and SNR values of at least 3 were considered to differentiate a true signal from background noise.

Data were normalized as follows:immunoglobulin positive control (IgG or IgA) values across all samples were averaged and the positive control value for each sample was divided by the mean positive control value to generate a normalization factor for each sample. Each signal was then multiplied by the normalization factor for each block (sample).

Extended Data

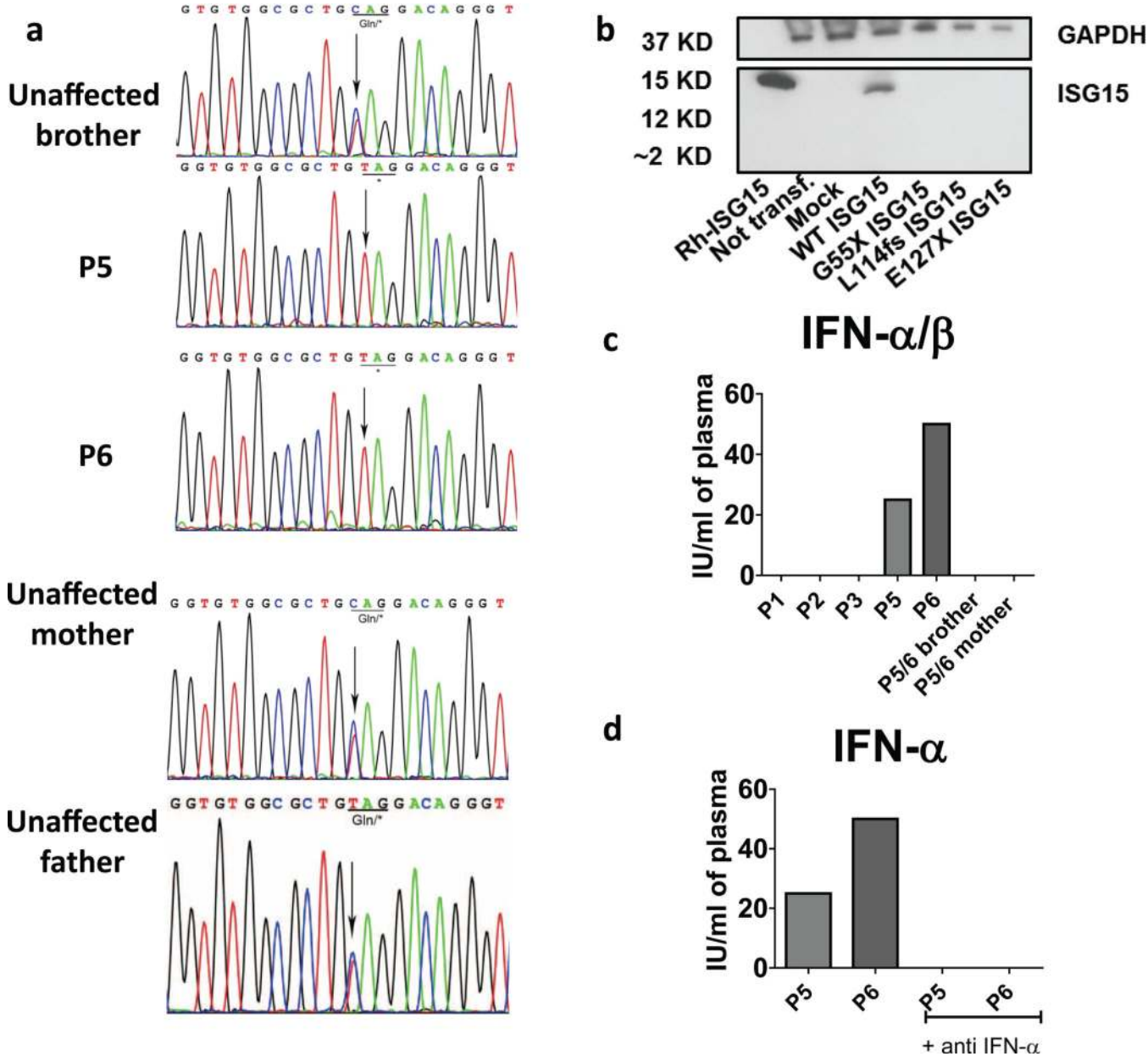

Extended Data Figure 1. Mutations in ISG15-deficient individuals, allele characterization and serum IFN-α concentrations

a, Sanger sequencing of *ISG15* exon 2 from genomic DNA in kindred C, with the variants highlighted. **b**, The wild type (WT) and three mutant alleles (G55X, L114fs, E127X- ISG15) were inserted into an expression vector and used to transfect HEK293T cells. Other HEK293T cells were mock-transfected (mock) or left untransfected (not transf.). The cell lysates isolated were subjected to western blotting, with recombinant human (Rh)-ISG15 used as a control. **c, d**, Plasma samples from P1, P2, P3, P5, P6 and the mother and brother of P5/6 were used in cytopathic protection assays, to measure antiviral activity (**c**) and

blocking antibodies against IFN-α were used to assess specificity (**d**) (experiment was performed one time).

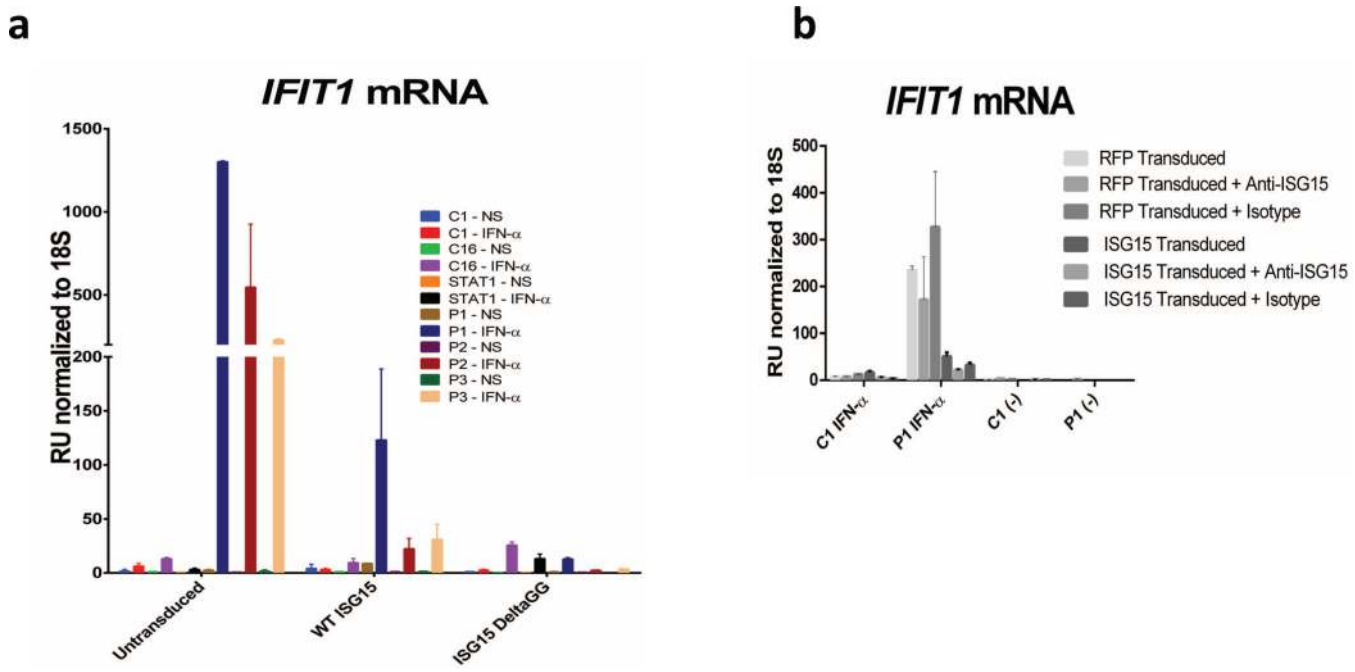

Extended Data Figure 2. A form of ISG15 that cannot be conjugated rescues the phenotype of ISG15-deficient cells

a, Lentiviral particles containing luciferase, wild-type (WT) *ISG15-RFP* or *ISG15*(Δ*GG*)-*RFP* genes were used to transduce hTert-immortalized fibroblasts from C1, a STAT1$^{-/-}$ subject, P1, P2 and P3. RFP-positive cells were obtained by sorting and were cultured for a few weeks. The cells were then treated with 1,000 IU of IFN-α2b for 12 h, washed with PBS and left to rest for 36 h, after which relative mRNA levels for *IFIT1* were determined. **b**, The experimental setting described in a was used in the presence or absence of vehicle control, anti-ISG15 antibodies or control IgG for luciferase and wild-type ISG15–RFP-transduced C1 and P1 hTert-immortalized fibroblasts (showing representative experiments with technical replicates and s.e.m., out of 3 performed).

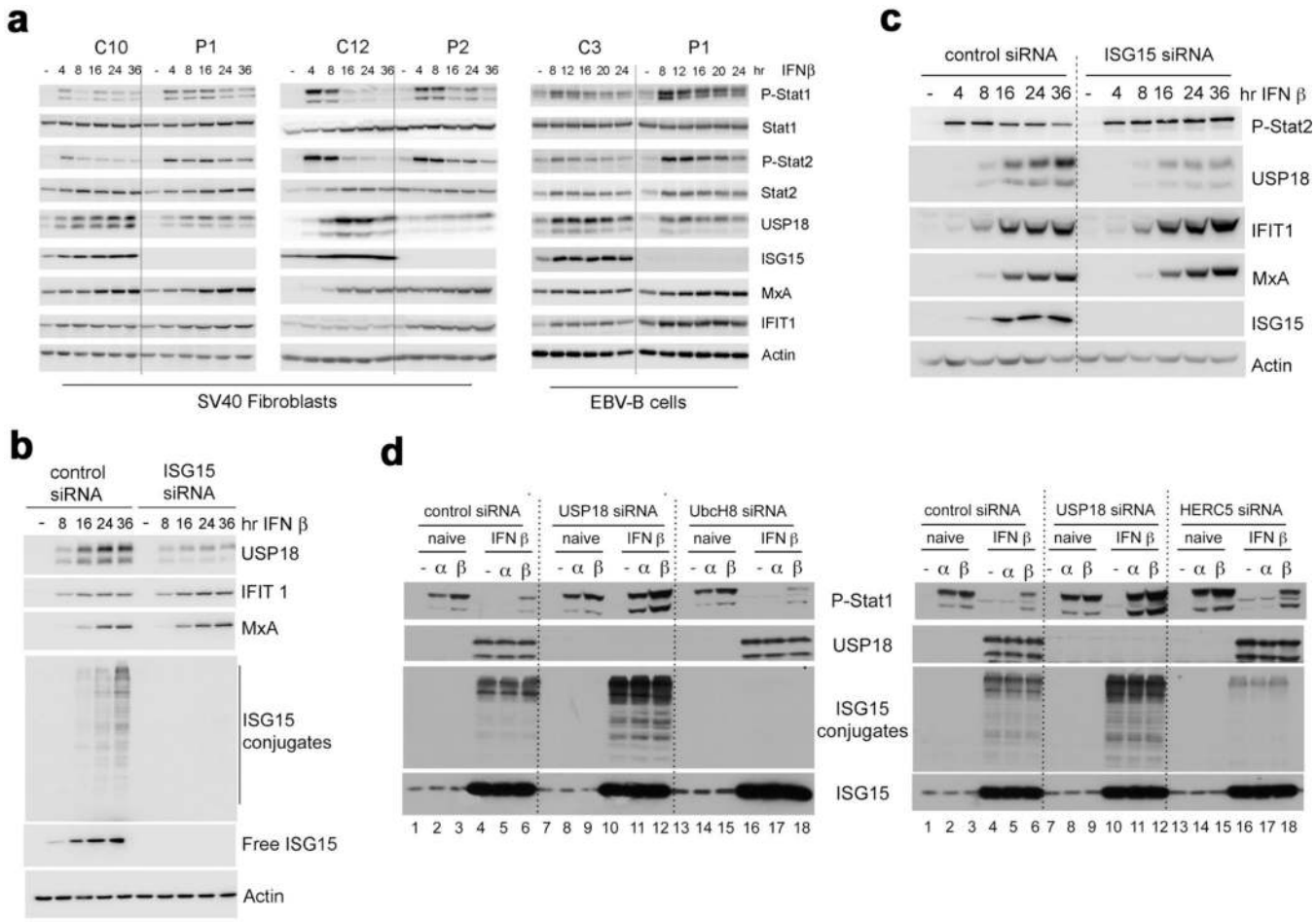

Extended Data Figure 3. Prolonged IFN signalling, low USP18, and high interferon-stimulated-gene-encoded protein levels in patient-derived cells and in ISG15-silenced human fibrosarcoma HLLR1-1.4 cells

a, Left panels, SV40-immortalized fibroblasts from two controls (C10 and C12) and two ISG15-deficient patients (P1 and P2) were stimulated with IFN-β (500 pM) for 4 to 36 h. Cell lysates (30 μg) were analysed with the indicated antibodies. Right, EBV-transformed B cells from control (C3) and patient P1 were stimulated with IFN-β for 8 to 24 h. Cell lysates (30 μg) were analysed with the indicated antibodies. **b**, HLLR1-1.4 cells were transfected with control siRNA or *ISG15* siRNA. One day post-transfection, IFN-β (500 pM) was added for various amounts of time. Cell lysates (30 μg) were analysed with the indicated antibodies (MxA and MX1 are used synonymously). **c**, WISH cells were stimulated and lysates analysed as described in **b. d**, HLLR1-1.4 cells were transfected with control siRNA, *USP18* siRNA and *UbcH8* (also known as *UBE2E2*) siRNA (left) or control siRNA, *USP18* siRNA and *HERC5* siRNA (right). One day post-transfection, cells were left untreated (naive) or were primed for 8 h with IFN-β (500 pM). Cells were washed and left to rest for 16 h before being pulsed for 30 min with 100pM IFN-α2 or IFN-β. Cell lysates (30 μg) were analysed with the indicated antibodies.

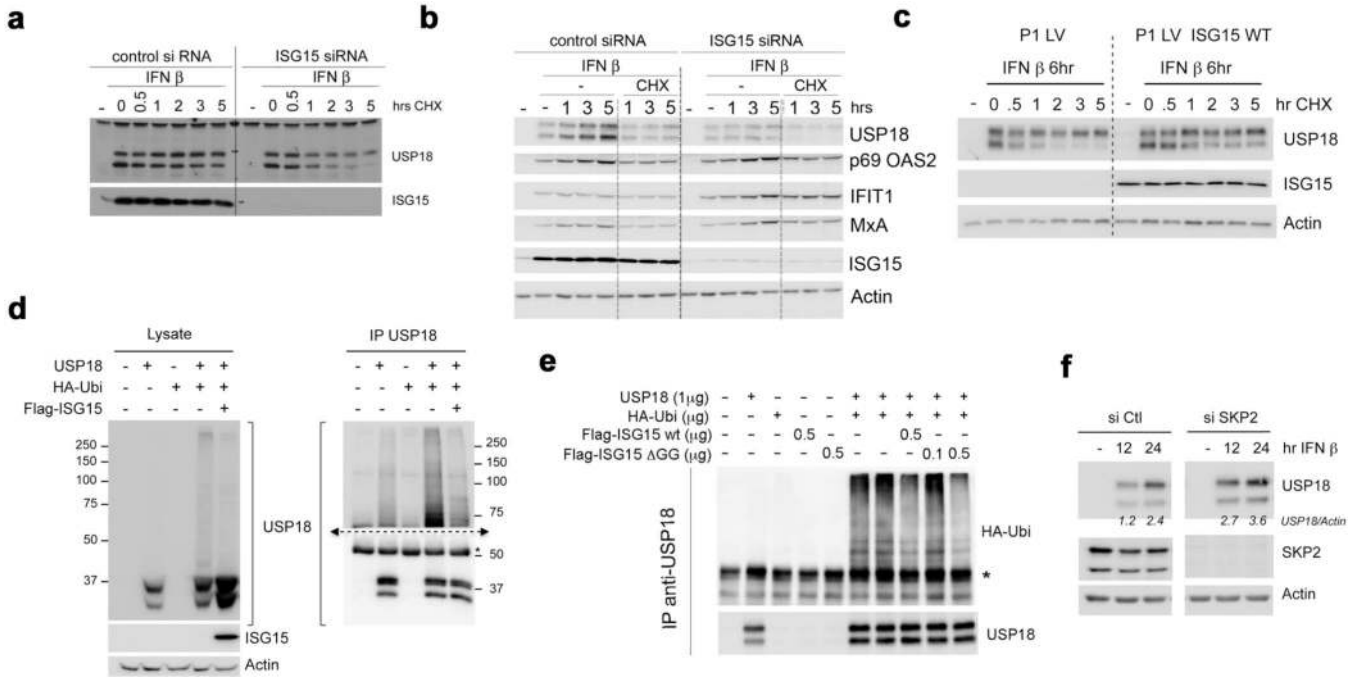

Extended Data Figure 4. ISG15 controls the stability of the USP18 protein, but not of other interferon-stimulated-gene products

a, HLLR1-1.4 cells were transfected with either control siRNA or *ISG15* siRNA. One day post-transfection, cells were stimulated with IFN-β (500 pM) for 6 h. Cycloheximide (CHX, 20 μgml^{-1}) was then added for various time periods, from 30 min to 5 h. Cell lysates (30 μg) were analysed with the indicated antibodies. **b**, As in **a**, with additional controls, cells treated with IFN only. Several interferon-stimulated genes were analysed. **c**, hTert-immortalized fibroblasts from patient P1 transduced with lentiviral particles expressing RFP and luciferase and wild-type ISG15 (LV ISG15 WT) were stimulated with IFN-β (500 pM) for 6 h. CHX was then added for the indicated times. Cell lysates (15 μg) were analysed by western blotting. **d**, HEK293T cells were transfected with USP18, HA–ubiquitin and Flag–ISG15 as indicated. Two days later, cells were lysed in modified RIPA buffer, USP18 was immunoprecipitated (IP) and analysed with anti-USP18 antibodies. Left panels, cell lysates (30 μg) were analysed by western blot with the indicated antibodies. Right panels, the immunoprecipitates were gel separated and transferred onto a membrane. The membrane was cut into two parts above the 50 kDa marker, both of which were blotted with anti-USP18 antibodies. The top part was exposed for 2 min, the bottom part for 20 s. Asterisk indicates IgG heavy chain. **e**, HEK293T cells were transfected with 1 μg of the USP18 construct alone or with 1 μg of HA– ubiquitin, in the presence or absence of Flag-tagged ISG15, either wild type or a mutant form of ISG15 that cannot be conjugated as it lacks the two carboxyterminal glycine residues (Flag–ISG15(ΔGG)). Two days later, cells were lysed in modified RIPA buffer, USP18 was immunoprecipitated and analysed with anti-HA or anti-USP18 antibodies. Asterisk indicates IgG heavy chain. **f**, hTert-immortalized fibroblasts from patient P3 were transfected with control siRNA or *SKP2* siRNA. We added IFN-β (500 pM) 24 h later and the cells were incubated for the indicated times. Cell lysates were

analysed with the indicated antibodies and USP18 levels were determined as a function of actin levels.

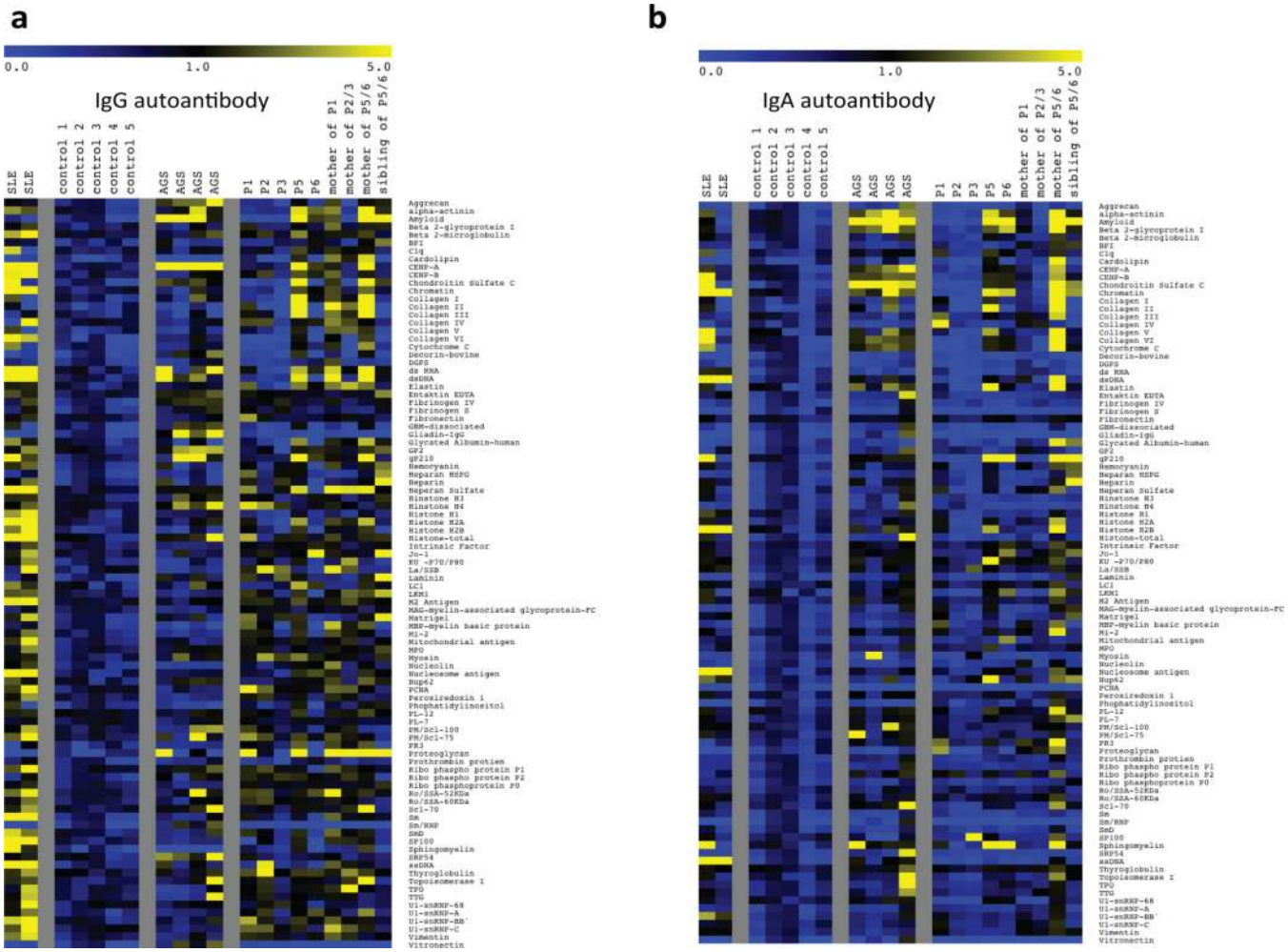

Extended Data Figure 5. Autoantibody development in ISG15-deficient individuals

a, b, Serum samples from ISG15-deficient, SLE and AGS patients were evaluated for the presence of IgG and IgA autoantibodies in a blinded experiment. Values for the negative control samples for each antigen were averaged and ratios of each sample to the mean for the negative controls plus 2 standard deviations were calculated, with values greater than 1 considered positive. A heat map of the ratio values was generated with MultiExperiment Viewer software (MeV, DFCI Boston, MA), with values coded as follows: 0, blue; 1, black; 5, yellow.

Extended Data Table 1

Patients have normal titres of antibodies against many viral antigens

Antibody responses								
	HAV	**EBV**	**Measles**	**VZV**	**CMV**	**HSV-1, HSV-2**	**Mumps**	**Influenza A**
Reference value	(<49%)	α-VCA IgG	(<70)	(mUI/ml <150)	(<0.6) IgG	(<1.1)	(<50)	(<30)
P1	NO	YES	NO	YES	YES	YES	N/A	YES
P2	N/A	YES	NO	NO	YES	NO	NO	YES
P3	YES	YES	NO	YES	YES	YES	YES	YES
P5	NO	NO	NO	NO	YES	NO	NO	NO
P6	NO	NO	YES	NO	YES	YES	NO	YES

YES= antibodies present

NO= antibodies not present

N/A= not done

Serum samples from patients and, when available, immediate family members, were tested for the presence of antibodies against hepatitis A virus (HAV), EBV, measles, varicella zoster virus (VZV), cytomegalovirus (CMV), herpes simplex viruses 1 and 2 (HSV-1 and HSV-2), mumps and influenza A viruses. NA, not available; YES, antibodies present; NO, antibodies not present. α-VCA IgG denotes anti EBV capsid antibodies.

Extended Data Table 2

Whole-exome sequencing results for patients with putative IBGC

		Whole Exome		
		P5	P6	P5/6 Mother
Nonsense (stop-gained)	Total	177	168	174
	Novel homozygous	1*	2*	0
	Novel heterozygous	7	5	5
Readthrough (stop-lost)	Total	78	77	74
	Novel homozygous	0	0	0
	Novel heterozygous	1	1	1
Missense	Total	11104	10967	11352
	Novel homozygous	8	17	9
	Novel heterozygous	210	204	234
Silent	Total	9848	9721	10065
	Novel homozygous	6	9	1
	Novel heterozygous	97	92	99
Frameshift	Total	178	168	178
	Novel homozygous	0	0	0
	Novel heterozygous	4	3	4
Inframe	Total	163	156	153
	Novel homozygous	2	2	0
	Novel heterozygous	3	1	2
UTR	Total	8508	8331	10131
	Novel homozygous	15	22	29
	Novel heterozygous	117	127	137
Splice	Total	3071	3067	3181
	Novel homozygous	6	5	1
	Novel heterozygous	41	42	39
ncRNA	Total	345	319	356
	Novel homozygous	1	1	0
	Novel heterozygous	3	4	3

Genomic DNA from the patients was used for massively parallel sequencing and the analysis (described in Methods) yielded the variants reported above. Asterisks denotes coding mutations reported in the main text. ncRNA, non-coding RNA; UTR, untranslated region.

Extended Data Table 3

Homozygous variants of genes other than ISG15 present in P1, P2, P5 and P6

P1	P2	P5	P6
SRP19	C1orf101	AIF1	APOBEC4
	GAB4	ALS2CR11	C19orf55

P1	P2	P5	P6
	MLL3	C19orf55	DEFB136
	PIK3CB	HLA-DRB5	KAZN
	THUMPD2	LILRA3	KDM4B
	ZC4H2	LST1	LRRFIP2
		MUC16	MGAM
		PRDX2	MUC16
		ZC3H12B	PADI4
			PLEKHN1
			PLXNB3
			PRDX2
			SMCR7
			TAS1R2
			TAS2R60
			TIAM2

Homozygous nonsense and missense variations from the four patients that were not present in the 1000 Genomes, EVS or dbSNP databases.

Extended Data Table 4

ISG15-deficient hTert fibroblasts have enhanced responses to IFN-α

No.	Fold Change	ANOVA p-value	FDR p-value	Gene Symbol	Description	Group
1	25.05	0.04796	0.788081	COLEC12	collectin sub-family member 12	Coding
2	11.72	0.000829	0.570142	---	ensembl_havana_lincrna:lincRNA c	Coding
3	8.97	0.025411	0.765877	---	accn=AK093732 class=mRNAlike lnc	NonCoding
4	7.73	0.025123	0.765877	---	accn=AK057151 class=mRNAlike lnc	NonCoding
5	6.95	0.044472	0.781343	HTRA3	HtrA serine peptidase 3	Coding
6	6.88	0.005831	0.665451	---	accn=DQ470079 class=mRNAlike lnc	NonCoding
7	6.66	0.000225	0.523843	SNORD114-	small nucleolar RNA, C/D box 114-2	Coding
8	6.59	0.020343	0.758127	RSAD2	radical S-adenosyl methionine dor	Coding
9	6.42	0.015871	0.757325	---	accn=AF026942 class=mRNAlike lncl	NonCoding
10	6.16	0.047461	0.786588	---	linc-WDR7-7 chr18:+:52559874-5256	NonCoding
11	6.13	0.008562	0.68638	IFI27	interferon, alpha-inducible protein	Coding
12	5.78	0.00754	0.682518	---	accn=AJ294851 class=mRNAlike lncl	NonCoding
13	5.52	0.000091	0.435886	---	accn=NR_030672 class=lncRNA nam	NonCoding
14	5.08	0.016151	0.757325	---	Positive Housekeeping Controls - P	Other
15	5.06	0.021768	0.758383	---	accn=NULL class=lncRNA name= ref	NonCoding
16	4.9	0.017117	0.758127	OAS3	2'-5'-oligoadenylate synthetase 3, 1	Coding
17	4.71	0.004252	0.650281	IFI44	interferon-induced protein 44	Coding
18	4.66	0.00854	0.68638	---	accn=AJ303364 class=mRNAlike lncl	NonCoding
19	4.58	0.018461	0.758127	OAS1	2'-5'-oligoadenylate synthetase 1, 4	Coding
20	4.52	0.005169	0.650281	TLR3	toll-like receptor 3	Coding
21	4.52	0.002347	0.641309	OASL	2'-5'-oligoadenylate synthetase-like	Coding
22	4.38	0.033644	0.775063	ZNF608	zinc finger protein 608	Coding
23	4.23	0.018847	0.758127	---	linc-CBR1-1 chr21:+:37377635-3737	NonCoding
24	4.16	0.007073	0.67996	---	accn=NR_037687 class=lncRNA nam	NonCoding
25	4.01	0.000633	0.570142	---	accn=NULL class=lincRNA name=Hu	NonCoding
26	3.95	0.041228	0.775063	NDNF	neuron-derived neurotrophic facto	Coding
27	3.82	0.018711	0.758127	SLCO2A1	solute carrier organic anion transpc	Coding
28	3.82	0.010603	0.72494	NOVA1	neuro-oncological ventral antigen 1	Coding
29	3.7	0.035475	0.775063	HERC6	HECT and RLD domain containing E3	Coding
30	3.51	0.029036	0.772054	NRN1	neuritin 1	Coding
31	3.46	0.015614	0.757325	---	havana:lincRNA chromosome:GRCh	Coding
32	3.46	0.022994	0.759536	MX1	myxovirus (influenza virus) resistar	Coding
33	3.41	0.022783	0.758383	EPB41L3	erythrocyte membrane protein ban	Coding
34	3.4	0.014995	0.754201	DHX58	DEXH (Asp-Glu-X-His) box polypept	Coding
35	3.39	0.01101	0.729998	PLXNC1	plexin C1	Coding
36	3.39	0.014229	0.743786	GDF5	growth differentiation factor 5	Coding
37	3.37	0.008001	0.684489	DCLK1	doublecortin-like kinase 1	Coding
38	3.16	0.012124	0.738151	MX2	myxovirus (influenza virus) resistar	Coding
39	3.14	0.027568	0.765877	---	accn=DQ914956 class=mRNAlike lnc	NonCoding
40	3.12	0.012473	0.739668	USP18	ubiquitin specific peptidase 18	Coding
41	3.08	0.018572	0.758127	DDX58	DEAD (Asp-Glu-Ala-Asp) box polyp	Coding
42	3.06	0.03665	0.775063	IFI35	interferon-induced protein 35	Coding
43	3.04	0.045433	0.783121	IL1R1	interleukin 1 receptor, type I	Coding
44	2.99	0.016966	0.758127	USP41	ubiquitin specific peptidase 41	Coding
45	2.98	0.03053	0.775063	LRRC32	leucine rich repeat containing 32	Coding
46	2.77	0.015518	0.756307	DDX60L	DEAD (Asp-Glu-Ala-Asp) box polyp	Coding
47	2.7	0.027738	0.765877	---	linc-COL1A2-2 chr7:+:93652144-936	NonCoding
48	2.67	0.018424	0.758127	---	accn=AL049990 class=mRNAlike lncl	NonCoding
49	2.67	0.000091	0.435886	KIAA1324L	KIAA1324-like	Coding
50	2.66	0.011206	0.731959	KCNA4	potassium voltage-gated channel, s	Coding
51	2.59	0.0137	0.741338	IFIT1	interferon-induced protein with te	Coding
52	2.56	0.007034	0.67996	SAMHD1	SAM domain and HD domain 1	Coding
53	2.53	0.045909	0.783121	SNED1	sushi, nidogen and EGF-like domair	Coding
54	2.5	0.0122	0.738151	---	accn=AK311114 class=mRNAlike lnc	NonCoding
55	2.43	0.033812	0.775063	---	havana:lincRNA chromosome:GRCh	Coding
56	2.43	0.020752	0.758127	SECTM1	secreted and transmembrane 1	Coding
57	2.39	0.042614	0.7768	PARP12	poly (ADP-ribose) polymerase fami	Coding
58	2.36	0.006938	0.67996	---	accn=NULL class=lncRNA name= ref	NonCoding
59	2.34	0.031174	0.775063	---	M35980,uc011gjx.2	Coding
60	2.33	0.001283	0.613989	---	DQ593902,uc021tyq.1	Coding
61	2.32	0.022003	0.758383	KCNJ15	potassium inwardly-rectifying chan	Coding
62	2.26	0.006149	0.674842	---	Negative Housekeeping Controls - I	Other
63	2.25	0.022299	0.758383	PPL	periplakin	Coding
64	2.23	0.030911	0.775063	SELENBP1	selenium binding protein 1	Coding
65	2.23	0.045121	0.783042	KIT	v-kit Hardy-Zuckerman 4 feline sarc	Coding
66	2.23	0.033234	0.775063	CPE	carboxypeptidase E	Coding
67	2.22	0.016735	0.758127	SP110	SP110 nuclear body protein	Coding
68	2.2	0.004368	0.650281	RFX8	regulatory factor X, 8	Coding
69	2.14	0.045843	0.783121	HLA-DRB1	major histocompatibility complex,	Coding
70	2.13	0.042907	0.7768	---	ncrna:snoRNA chromosome:GRCh3	Coding
71	2.08	0.027865	0.765877	PITPNC1	phosphatidylinositol transfer prote	Coding
72	2.06	0.011247	0.731959	RXFP1	relaxin/insulin-like family peptide	Coding
73	2.06	0.024753	0.765425	---	accn=AY665470 class=mRNAlike lncl	NonCoding
74	2.05	0.03305	0.775063	CYYR1	cysteine/tyrosine-rich 1	Coding
75	2.03	0.030124	0.775063	ARHGEF3	Rho guanine nucleotide exchange f	Coding
76	2.02	0.023303	0.759536	---	linc-CNTNAP3B-1 chr9:+:43313920-4	NonCoding
77	2.01	0.005787	0.665451	NMI	N-myc (and STAT) interactor	Coding
78	2.01	0.003072	0.644953	---	accn=NULL class=lincRNA name=Hu	NonCoding
79	-2.01	0.048814	0.791563	---	BC022047,uc003pyw.1	Coding
80	-2.01	0.003758	0.647229	ACO1	aconitase 1, soluble	Coding
81	-2.03	0.048774	0.791314	ATP10D	ATPase, class V, type 10D	Coding
82	-2.05	0.01095	0.729998	---	accn=AF086045 class=mRNAlike lncl	NonCoding
83	-2.07	0.02484	0.765425	---	accn=DQ004397 class=mRNAlike lnc	NonCoding
84	-2.08	0.000915	0.570142	---	DQ586227,uc001zzt.2	Coding
85	-2.1	0.040285	0.775063	---	accn=NULL class=lincRNA name=Hu	NonCoding
86	-2.1	0.021565	0.758383	---	Negative Housekeeping Controls - I	Other
87	-2.14	0.036392	0.775063	NTN4	netrin 4	Coding
88	-2.15	0.00482	0.650281	HOXC9	homeobox C9	Coding
89	-2.16	0.000139	0.435886	---	accn=NULL class=lincRNA name=Hu	NonCoding
90	-2.19	0.001455	0.625179	CDR1	cerebellar degeneration-related pr	Coding
91	-2.25	0.016418	0.758127	---	Negative Housekeeping Controls - I	Other
92	-2.26	0.027323	0.765877	LTBP2	latent transforming growth factor b	Coding
93	-2.27	0.019149	0.758127	---	linc-PIK3CG-3 chr7:+:106264517-106	NonCoding
94	-2.27	0.043332	0.778351	SLC38A1	solute carrier family 38, member 1	Coding
95	-2.29	0.008635	0.68638	LOC90784	uncharacterized LOC90784	Coding
96	-2.31	0.031712	0.775063	HSBP1L1	heat shock factor binding protein 1-	Coding
97	-2.32	0.019638	0.758127	BAIAP2L1	BAI1-associated protein 2-like 1	Coding
98	-2.36	0.02371	0.759536	TMEM130	transmembrane protein 130	Coding
99	-2.37	0.013599	0.741338	---	accn=S77359 class=mRNAlike lncRN	NonCoding
100	-2.38	0.000814	0.570142	---	ncrna:lincRNA chromosome:GRCh3	Coding
101	-2.47	0.000151	0.435886	---	linc-EPHA6-1 chr3:+:96336028-9633	NonCoding
102	-2.5	0.024874	0.765425	SH3BGRL2	SH3 domain binding glutamic acid-r	Coding
103	-2.52	0.001499	0.625613	---	accn=NR_028343 class=lncRNA nam	NonCoding
104	-2.57	0.005854	0.665451	PPP1R3C	protein phosphatase 1, regulatory s	Coding
105	-2.61	0.041643	0.775063	---	accn=NR_024179 class=lncRNA nam	NonCoding
106	-2.67	0.003801	0.647229	ZNF415	zinc finger protein 415	Coding
107	-2.82	0.028784	0.770664	---	AK124511,uc003jyj.1	Coding
108	-2.89	0.001615	0.636575	---	accn=AK001007 class=mRNAlike lnc	NonCoding
109	-2.89	0.026776	0.765877	SLC30A4	solute carrier family 30 (zinc transp	Coding
110	-2.91	0.010608	0.72494	DCLK2	doublecortin-like kinase 2	Coding
111	-3.04	0.042969	0.7768	TGFB2	transforming growth factor, beta 2	Coding
112	-3.15	0.046017	0.783121	IGFBP7	insulin-like growth factor binding p	Coding
113	-3.2	0.020952	0.758127	PLCB4	phospholipase C, beta 4	Coding
114	-3.53	0.011009	0.729998	---	accn=NR_036614 class=lncRNA nam	NonCoding
115	-3.64	0.001799	0.641309	---	DQ583712,uc022bav.1	Coding
116	-3.74	0.040415	0.775063	---	Positive Housekeeping Controls - P	Other
117	-4.09	0.039055	0.775063	---	accn=AF540057 class=mRNAlike lncl	NonCoding
118	-4.31	0.008198	0.684489	COL4A2	collagen, type IV, alpha 2	Coding
119	-4.42	0.039009	0.775063	HOXC11	homeobox C11	Coding
120	-5.29	0.009866	0.710704	---	accn=X05562 class=mRNAlike lncRN	NonCoding
121	-5.62	0.034432	0.775063	SERPINB7	serpin peptidase inhibitor, clade B	Coding
122	-6.57	0.000376	0.551172	HOXC10	homeobox C10	Coding
123	-6.82	0.009785	0.710704	COL4A1	collagen, type IV, alpha 1	Coding
124	-14.31	0.000866	0.570142	TRHDE	thyrotropin-releasing hormone deg	Coding

We treated hTert-immortalized fibroblasts from three controls and three patients with 1,000 IU IFN-α2b for 12 h. The cells were then washed three times with PBS and left to rest for an additional 36 h, after which we isolated mRNA for microarray analysis. We found that 124 transcripts were significantly different in patients, by a factor of more than two with respect to control cell lines, in statistical analyses based on ANOVA and false discovery rates.

Supplementary Material

Refer to Web version on PubMed Central for supplementary material.

Acknowledgements

The Laboratory of Human Genetics of Infectious Diseases is supported by grants from the French National Agency for Research (ANR), the EU grant HOMITB (HEALTH-F32008-200732), the St Giles Foundation, the National Center for Research Resources and the National Center for Advancing Sciences (NCATS), National Institutes of Health grant number 8UL1TR000043, the Rockefeller University, the National Institute of Allergy and Infectious Diseases grant number R37AI095983, Institut Merieux research grant and the Empire State StemCell fund through NYSDOH Contract #C023046 to Flow Cytometry Research Core at the Rockefeller University. The Cytokine Signaling Unit is supported by the Institut Pasteur, CNRS and INSERM. S.P. and G.U. received funding from the EU Seventh Framework Programme under grant agreement 223608. V.F.-N. was supported by the Ligue contre le Cancer. L.R. is a Human Frontier Science Program long-term fellow. L.D.N. was supported by the National Institute of Allergy and Infectious Diseases grant number 1PO1AI076210-01A1. Y.J.C. thanks the Manchester Biomedical Research Centre and the Greater Manchester Comprehensive Local Research Network, the European Union's Seventh Framework Programme (FP7/2007-2013) under grant agreement 241779, and the European Research Council (GA 309449). A.G.-S. acknowledges NIAID grants U19AI083025 and P01AI090935 for support. We thank C. Daussy for technical assistance, E. Bianchi and F. Michel for discussions. We thank D. Zhang and the members of the Zhang laboratory for assistance, advice and discussions. This work was supported by Chinese National Natural Science Foundation grants (81000079, 81170165) to X.Z. D.B. is supported by the National Institute of Allergy and Infectious Diseases grant number R00AI106942-02.

Microarray data have been deposited in the Gene Expression Omnibus under accession number GSE60359; WES data have been deposited in the BioProject database under accession number PRJNA167660.

References

1. Jeon YJ, Yoo HM, Chung CH. ISG15and immune diseases. Biochim. Biophys. Acta. 2010; 1802:485–496. [PubMed: 20153823]
2. Morales DJ, Lenschow DJ. The antiviral activities of ISG15. J. Mol. Biol. 2013; 425:4995–5008. [PubMed: 24095857]
3. Skaug B, Chen ZJ. Emerging role of ISG15 in antiviral immunity. Cell. 2010; 143:187–190. [PubMed: 20946978]
4. Zhang D, Zhang DE. Interferon-stimulated gene 15 and the protein ISGylation system. J. Interferon Cytokine Res. 2011; 31:119–130. [PubMed: 21190487]
5. Bogunovic D, et al. Mycobacterial disease and impaired IFN-γ immunity in humans with inherited ISG15 deficiency. Science. 2012; 337:1684–1688. [PubMed: 22859821]
6. Baechler EC, et al. Interferon-inducible gene expression signature in peripheral blood cells of patients with severe lupus. Proc. Natl Acad. Sci.USA. 2003; 100:2610–2615. [PubMed: 12604793]
7. Crow YJ. Aicardi–Goutières syndrome. Handb. Clin. Neurol. 2013; 113:1629–1635. [PubMed: 23622384]
8. Crow YJ, Rehwinkel J. Aicardi–Goutières syndrome and related phenotypes: linking nucleic acid metabolism with autoimmunity. Hum. Mol. Genet. 2009; 18:R130–R136. [PubMed: 19808788]
9. Rice GI, et al. Assessment of interferon-related biomarkers in Aicardi–Goutières syndrome associated with mutations in *TREX1, RNASEH2A, RNASEH2B, RNASEH2C, SAMHD1*, and *ADAR*: a case–control study. Lancet Neurol. 2013; 12:1159–1169. [PubMed: 24183309]
10. Malakhova OA, et al. UBP43 is a novel regulator of interferon signaling independent of its ISG15 isopeptidase activity. EMBO J. 2006; 25:2358–2367. [PubMed: 16710296]
11. Tokarz S, et al. The ISG15 isopeptidase UBP43 is regulated by proteolysis via the SCFSkp2 ubiquitin ligase. J. Biol. Chem. 2004; 279:46424–46430. [PubMed: 15342634]
12. Kendall B, Cavanagh N. Intracranial calcification in paediatric computed tomography. Neuroradiology. 1986; 28:324–330. [PubMed: 3463882]
13. Livingston JH, Stivaros S, van der Knaap MS, Crow YJ. Recognizable phenotypes associated with intracranial calcification. Dev. Med. Child Neurol. 2013; 55:46–57. [PubMed: 23121296]

14. Manyam BV. What is and what is not 'Fahr's disease'. Parkinsonism Relat. Disord. 2005; 11:73–80. [PubMed: 15734663]
15. Wang C, et al. Mutations in *SLC20A2* link familial idiopathic basal ganglia calcification with phosphate homeostasis. Nature Genet. 2012; 44:254–256. [PubMed: 22327515]
16. Keller A, et al. Mutations in the gene encoding PDGF-B cause brain calcifications in humans and mice. Nature Genet. 2013; 45:1077–1082. [PubMed: 23913003]
17. Nicolas G, et al. Mutation of the PDGFRB gene as a cause of idiopathic basal ganglia calcification. Neurology. 2013; 80:181–187. [PubMed: 23255827]
18. Briggs TA, et al. Tartrate-resistant acid phosphatase deficiency causes a bone dysplasia with autoimmunity and a type I interferon expression signature. Nature Genet. 2011; 43:127–131. [PubMed: 21217755]
19. Casanova JL, Abel L. Genetic dissection of immunity to mycobacteria: the human model. Annu. Rev. Immunol. 2002; 20:581–620. [PubMed: 11861613]
20. Casanova JL, Abel L. The genetic theory of infectious diseases: a brief history and selected illustrations. Annu. Rev. Genomics Hum. Genet. 2013; 14:215–243. [PubMed: 23724903]
21. Bogunovic D, Boisson-Dupuis S, Casanova JL. ISG15: leading a double life as a secreted molecule. Exp. Mol. Med. 2013; 45:e18. [PubMed: 23579383]
22. Bennett L, et al. Interferon and granulopoiesis signatures in systemic lupus erythematosus blood. J. Exp. Med. 2003; 197:711–723. [PubMed: 12642603]
23. Raymond AA, Zariah AA, Samad SA, Chin CN, Kong NC. Brain calcification in patients with cerebral lupus. Lupus. 1996; 5:123–128. [PubMed: 8743125]
24. Durfee LA, Lyon N, Seo K, Huibregtse JM. The ISG15 conjugation system broadly targets newly synthesized proteins: implications for the antiviral function of ISG15. Mol. Cell. 2010; 38:722–732. [PubMed: 20542004]
25. Broering R, et al. The interferon stimulated gene 15 functions as a proviral factor for the hepatitis C virus and as a regulator of the IFN response. Gut. 2010; 59:1111–1119. [PubMed: 20639253]
26. Chua PK, et al. Modulation of alpha interferon anti-hepatitis C virus activity by ISG15. J. Gen. Virol. 2009; 90:2929–2939. [PubMed: 19656964]
27. François-Newton V, et al. USP18-based negative feedback control is induced by type I and type III interferons and specifically inactivates interferon α response. PLoS ONE. 2011; 6:e22200. [PubMed: 21779393]
28. Francois-Newton V, Livingstone M, Payelle-Brogard B, Uze G, Pellegrini S. USP18 establishes the transcriptional and anti-proliferative interferon α/β differential. Biochem. J. 2012; 446:509–516. [PubMed: 22731491]
29. Frescas D, Pagano M. Deregulated proteolysis by the F-box proteins SKP2 and β-TrCP: tipping the scales of cancer. Nature Rev. Cancer. 2008; 8:438–449. [PubMed: 18500245]
30. Hertzog PJ, Williams BR. Fine tuning type I interferon responses. Cytokine Growth Factor Rev. 2013; 24:217–225. [PubMed: 23711406]
31. Li QZ, et al. Protein array autoantibody profiles for insights into systemic lupus erythematosus and incomplete lupus syndromes. Clin. Exp. Immunol. 2007; 147:60–70. [PubMed: 17177964]

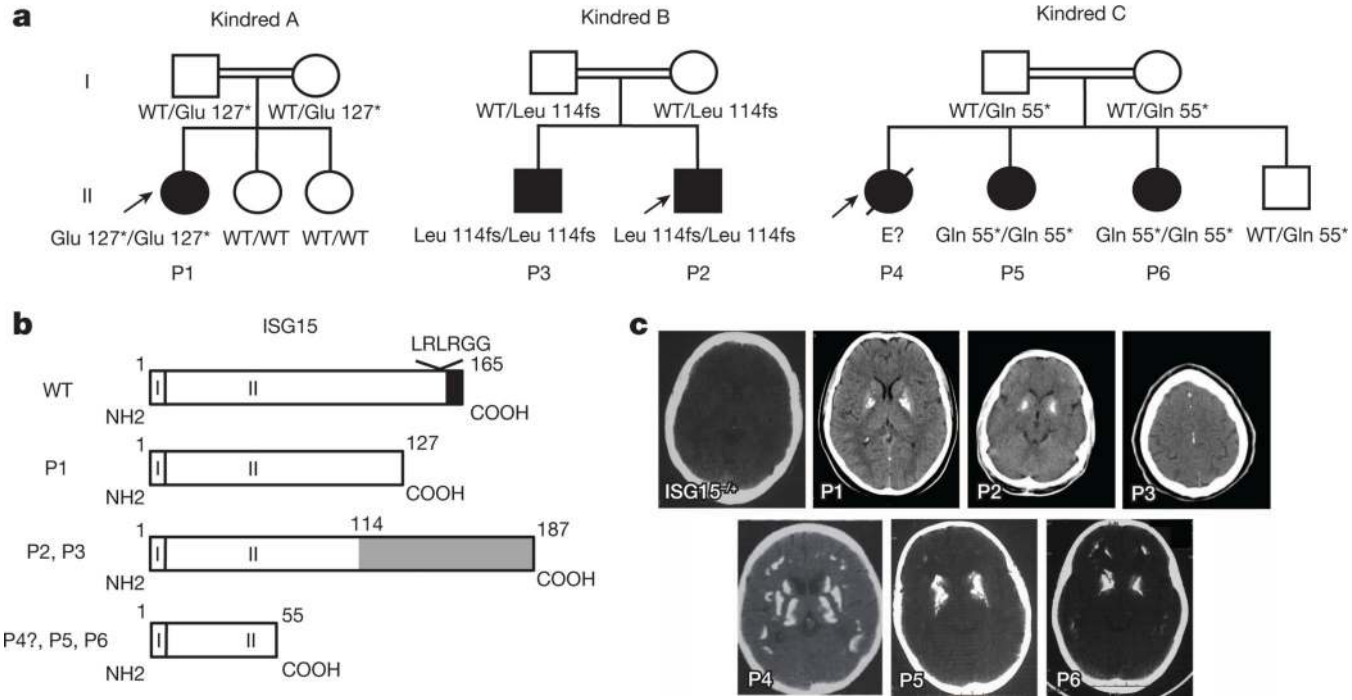

Figure 1. Familial segregation of the ISG15 allele and CT scans for the affected families

a, Familial segregation in a family from Turkey (Kindred A), a family from Iran (Kindred B) (previously reported) and a family from China (Kindred C). Asterisks denote stop codons; E denotes unknown genotype; fs, frameshift; WT, wild type. **b**, Graphical representation of the proISG15 protein, with the LRLRGG motif required for substrate ISGylation and the eight-amino-acid sequence (black) cleaved to yield ISG15, and the putative proteins synthesized in the patients. **c**, Axial view cerebral CT scans of P1, P2, P3, P4, P5, P6 and the healthy mother of P4, P5 and P6 ($ISG15^{-/+}$).

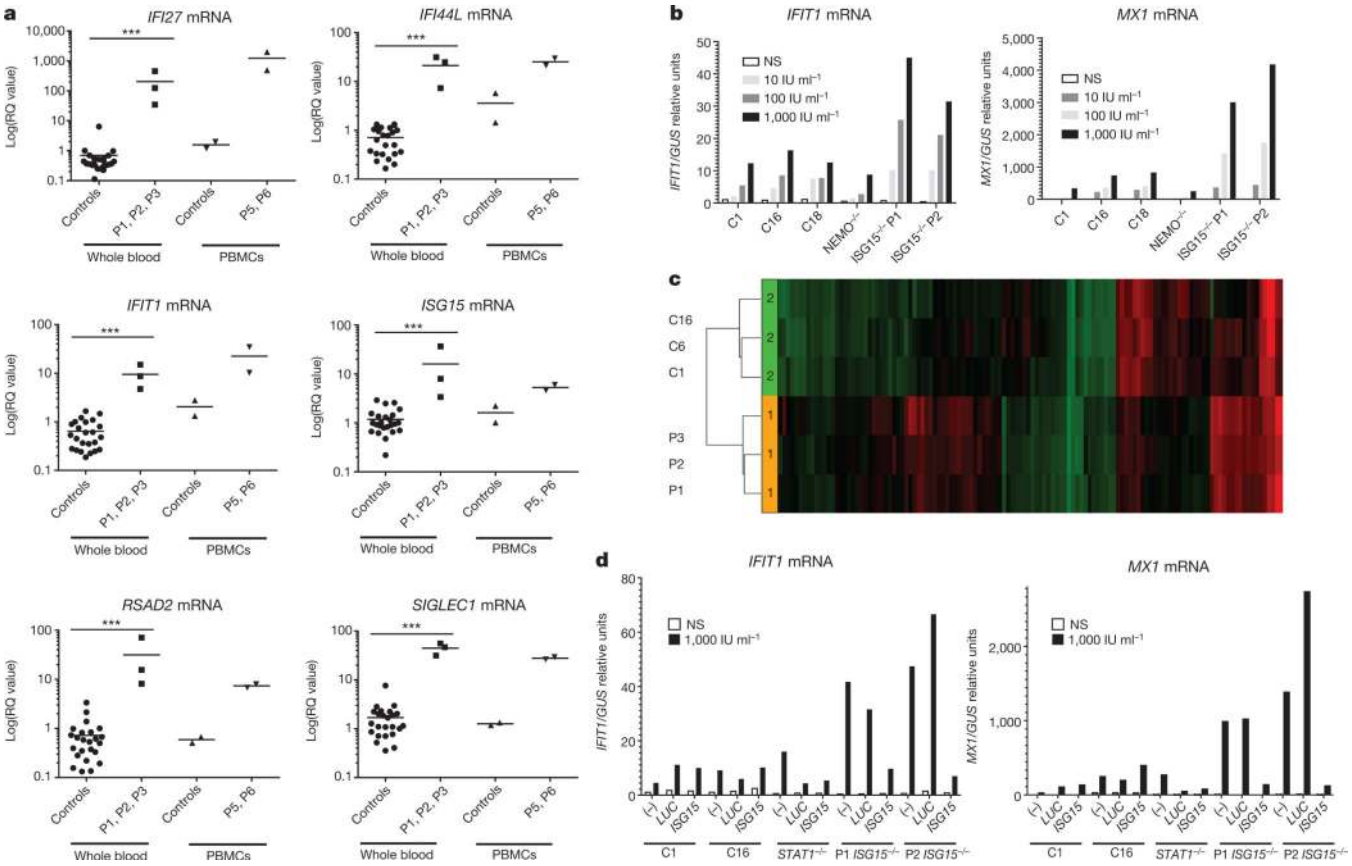

Figure 2. High levels of interferon-stimulated gene expression in ISG15-deficient individuals

a, Relative mRNA levels for *IFI27, IFI44L, IFIT1, ISG15, RSAD2* and *SIGLEC1* in peripheral blood from patients ($n = 3$) or controls (C) ($n = 24$) or in peripheral blood mononuclear cells (PBMCs) from family members (wild type and heterozygous for ISG15 deficiency) ($n = 2$) and patients ($n = 2$), as assessed by RT–qPCR, comparison done with unpaired *t*-tests. ***$P < 0.0001$; horizontal bars represent means; RQ defined in reference to C1 unstimulated condition. **b**, hTert-immortalized fibroblasts from C1, C16, C18, a NEMO$^{-/-}$ subject (as a negative control due to known hyporesponsiveness), P1 and P2 were treated with the indicated doses of IFN-α2b for 12 h, washed with PBS and left to rest for 36 h, after which relative mRNA levels were assessed. **b** shows a representative experiment of three performed. *GUS* is used as a housekeeping control gene. NS, not stimulated. **c**, The same experimental procedure as in **b** was followed, but the mRNA was used for a microarray experiment, for C1, C6, C16, P1, P2 and P3 cells, with green indicating relative upregulation and red indicating downregulation of the probe concerned. **d**, In the same experimental setup, we used lentiviral particles containing luciferase–RFP (red fluorescent protein) or wild-type ISG15–RFP genes to transduce hTert-immortalized fibroblasts and then assessed mRNA levels for *IFIT1* and *MX1* by RT–qPCR. Panel **d** shows one representative experiment of three performed, where (–) denotes not transduced conditions.

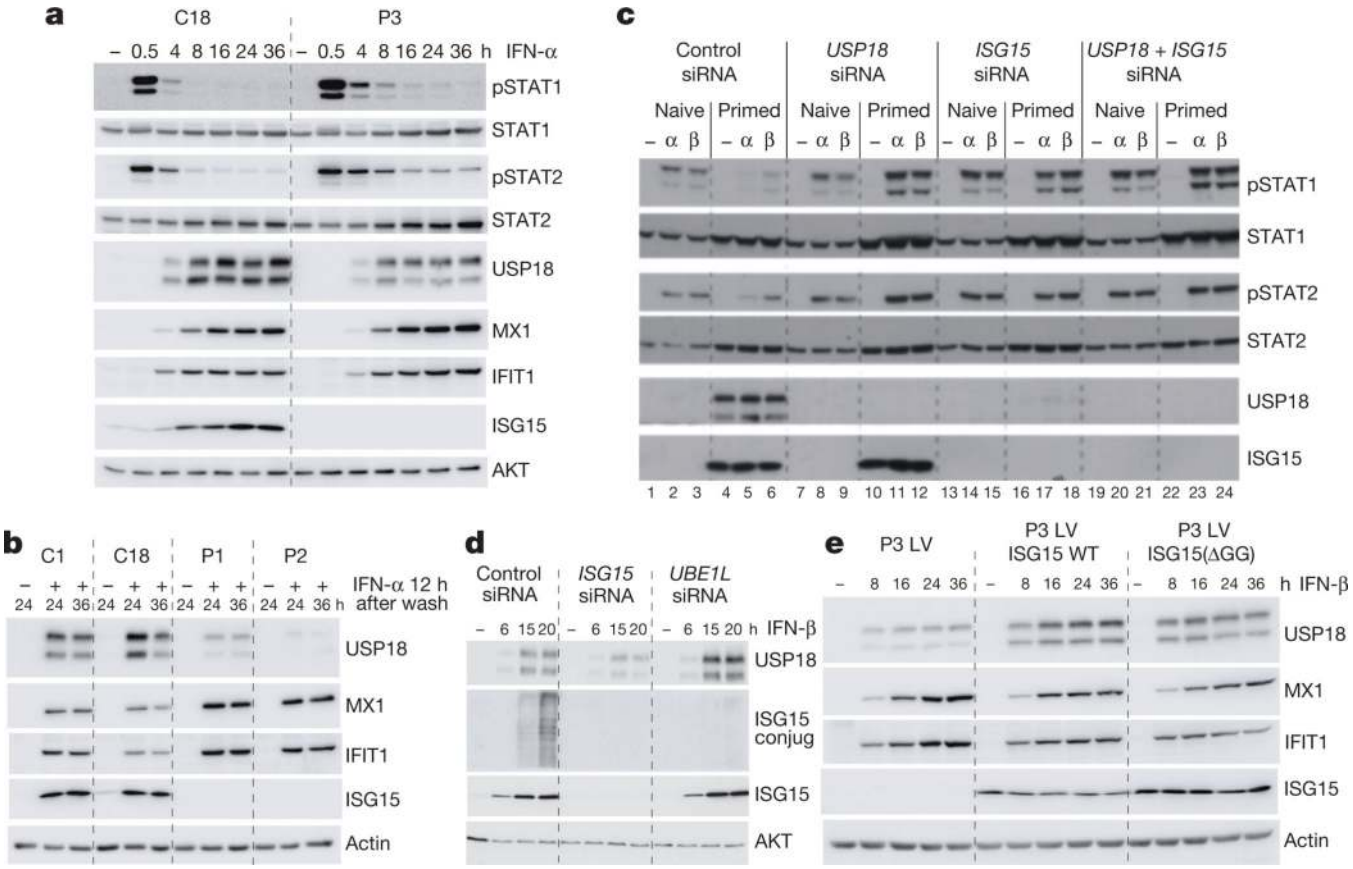

Figure 3.

a, hTert-immortalized fibroblasts from a control (C18) and patient P3 were treated with 100pM IFN-α2 for 0.5 to 36 h. Cell lysates were analysed by western blot for levels of phosphorylated STAT (pSTAT) proteins and proteins encoded by interferon-stimulated genes. **b**, hTert-immortalized fibroblasts from controls (C1, C18) and patients P1 and P2 were treated with 100pM IFN-α2 for 12 h, washed and left to rest for 24 or 36 h. Protein levels were assessed by western blot. **c**, HLLR1-1.4 cells were transfected with control short interfering RNA (siRNA) or with siRNA targeting *USP18, ISG15* or both. One day later, cells were left untreated (naive) or were primed for 8 h with 500 pM IFN-β, washed and left to rest for 16 h, and then restimulated for 30 min with 100 pM IFN-α2or IFN-β. Lysates were analysed with the indicated antibodies. **d**, HLLR1-1.4 cells were transfected with control siRNA, *ISG15* siRNA or *UBE1L* siRNA. One day later, IFN-β (500 pM) was added for various periods of time. Lysates were analysed as indicated. **e**, hTert-immortalized fibroblasts from P3 transduced with lentiviral particles expressing RFP and luciferase (LV), wild-type ISG15 (LV ISG15 WT) or the IS15(ΔGG) mutant (LV ISG15(ΔGG)) were stimulated with IFN-β (500 pM) for 8 to 36 h and protein levels assessed by western blot.

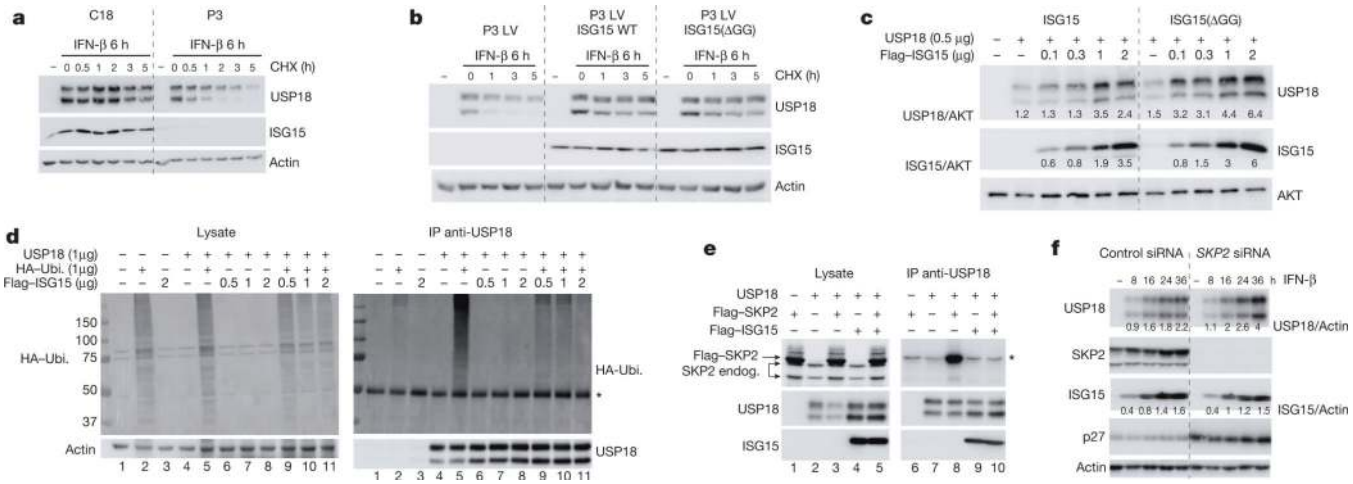

Figure 4. Free ISG15 stabilizes USP18 by preventing SKP2-dependent ubiquitination

a, hTert-immortalized fibroblasts from control (C18) and patient P3 were left untreated (–) or treated for 6 h with IFN-β (500 pM). Cycloheximide (CHX) was added for an additional 0.5 to 5 h. Lysates were analysed as indicated. **b**, hTert fibroblasts from P3 transduced with lentiviral particles expressing RFP and luciferase (LV) conjugated to wild-type ISG15 (LV ISG15 WT) or the non-conjugatable ISG15(ΔGG) mutant (LV ISG15(ΔGG)) were processed as in **a. c**, HEK293T cells were transfected with USP18 expression vector alone or in combination with various amounts of ISG15 (Flag–ISG15), either wild-type or ΔGG. Two days later, lysates were analysed as indicated. Ratios of USP18 or ISG15 to AKT are shown below gels. **d**, HEK293T cells were cotransfected with USP18 and haemagglutinin (HA)–ubiquitin in the presence of wild-type ISG15 (Flag–ISG15). Two days later, lysates were subjected to immunoprecipitation (IP) with anti-USP18 antibodies. Lysates (left panels) were analysed with antibodies against HA and actin. Immunoprecipitates (right panels) were analysed with antibodies against HA and USP18. Asterisk indicates IgG heavy chain. **e**, HEK293T cells were transfected with USP18, Flag–SKP2 and Flag–ISG15 expression vectors, as indicated. Two days later, USP18 was immunoprecipitated. Lysates (left panels) and immunoprecipitates (right panels) were analysed with antibodies against SKP2, USP18 and ISG15. Arrowheads indicate two endogenous SKP2 isoforms; arrow indicates ectopic Flag–SKP2; asterisk, background band (lanes 6, 7 and 9, 10). **f**, HLLR1-1.4 cells were transfected with control siRNA or *SKP2* siRNA and 24 h later IFN-β (500 pM) was added and cells were incubated for various times. Lysates were analysed as indicated. USP18 and ISG15 levels were quantified relative to actin levels.